Calibration of Mid-Frequency Aperture Array Stations Using Self-holography

Stefan J. Wijnholds*†

Abstract — **The stations (subarrays) of the Mid-Frequency Aperture Array (MFAA) system for the Square Kilometre Array (SKA) operating in the 450–1450 MHz range are envisaged to have $\sim 10^3$ to $\sim 10^4$ receive paths. This will make standard calibration procedures based on the array covariance matrix computationally expensive. In this paper, I therefore propose a method to calibrate the receive path gains during regular observations by correlating the signals from individual receive paths with the signal from a reference beam formed by the same station, i.e., "self-holography". I discuss the performance of this approach using simulations for a realistic MFAA scenario.**

1 INTRODUCTION

A Mid-Frequency Aperture Array (MFAA) system operating in the 450–1450 MHz range is envisaged to be constructed in South-Africa as part of the second phase of the Square Kilometre Array (SKA) [1, 2]. Its large instantaneous field-of-view (FoV, 100–200 sq. deg.) and observing capabilities provided by its multi-beaming ability will make this MFAA system an unprecedented transient monitoring and surveying instrument at these operating frequencies. The MFAA system is envisaged to consist of ~ 250 *stations* (subarrays) with a diameter somewhere between 40 and 60 m. These stations can either have a sparse irregular array layout or a dense regular configuration [3]. To meet the FoV requirement, the number of antennas that can be combined in a single *tile* using analog beamforming before digitization is limited. As a result, the number of receive paths within a station is expected to be $\sim 10^3$ to $\sim 10^4$.

Calibration needs to be an integral part of the system design to ensure that the system meets its expected performance. This also includes calibration of the complex valued receive path gains within a station. These are normally calibrated based on the array covariance matrix. Due to the large number of receive paths, such an approach will be computationally expensive (or even infeasible) for MFAA stations. A holographic measurement [4], in which the antennas to be calibrated are correlated with a reference signal, would reduce the number of correlations from $P(P-1)/2$ to $P+1$, where P is the number of receive paths in the array. In this paper, I propose a holographic calibration method using a reference beam formed by the station itself, which could be called *self-holography.* The disadvantage of self-holography is that there may be a significant unwanted correlation between the reference signal and the signals of the receive paths to be calibrated due to the fact that those same receive paths are used to provide the reference beam. I will analyse this effect and discuss its implications for system design and gain and noise power variations between receive paths.

*Netherlands Institute for Radio Astronomy (ASTRON), Oude Hoogeveensedijk 4, 7991 PD Dwingeloo, The Netherlands, e-mail: wijnholds@astron.nl, tel.: +31 521 595 261.

†Stellenbosch University, Department of Electrical and Electronic Engineering, Cnr Banghoek Road & Joubert Street, Stellenbosch 7600, South Africa

2 SELF-HOLOGRAPHY

2.1 Data model

The station consists of P tiles in which M antenna signals are combined by an analog beamformer such that there are $N = PM$ antennas in the station. The tile beams and reference beam are assumed to be pointed to a calibration source. All other source signals are assumed to be sufficiently suppressed by the reference beam to be ignored. For a specific frequency ν the geometric delay of the signal at the mth antenna in the pth tile can be described by the phasor $a_{p,m} = e^{2\pi j \nu \boldsymbol{\xi}_{p,m} \cdot \mathbf{l}}$, where $\boldsymbol{\xi}_{p,m}$ denotes the position of the element in Cartesian coordinates and $\mathbf{l}$ denotes the direction of the source in direction cosines. It is assumed that these phasors are exactly compensated by the tile beamformer, whose weights can thus be described as $w_{p,m} = a_{p,m}$. Stacking the weights for the pth tile in a $M \times 1$ vector $\mathbf{w}_p$, the delay phasors in a $M \times 1$ vector $\mathbf{a}_p$ and the noise signals from the receiving elements in a $M \times 1$ vector $\mathbf{n}_p(t)$, we can describe the signal from the pth tile as

$$\begin{aligned} x_p(t) &= g_p \mathbf{w}_p^H (\mathbf{a}_p s(t) + \mathbf{n}_p(t)) \\ &= g_p M s(t) + \mathbf{w}_p^H \mathbf{n}_p(t), \end{aligned} \qquad (1)$$

where g_p is the receive path gain for the pth tile that we need to calibrate and $s(t)$ is the signal from the calibration source, which is assumed to be uncorrelated with the noise signals. The noise signals are also assumed to be mutually uncorrelated. However, more complex noise structures can be incorporated in this model.

2.2 Self-holography

The signals from the P tiles can be stacked into a $P \times 1$ vector $\mathbf{x}(t)$. In the proposed self-holography method, a reference beam is formed from those signals by applying weights $\mathbf{w}_{\rm ref}$ to these signals to produce the reference beam signal

$$y(t) = \mathbf{w}_{\rm ref}^H \mathbf{x}(t). \quad (2)$$

This reference signal is then correlated with the signals from the individual tiles. The measured correlations can be stacked into a $P \times 1$ vector $\widehat{\mathbf{r}}$ whose expected value is

$$\begin{aligned} \mathbf{r} &= \mathcal{E}\left\{\mathbf{x}(t) y^H(t)\right\} \\ &= \mathbf{g}\left(\mathbf{g}^H \mathbf{w}_{\rm ref}\right) M^2 \sigma_{\rm cal} + M\sigma_{\rm n}\mathbf{w}_{\rm ref}, \end{aligned} \quad (3)$$

where $\mathbf{g}$ is the $P \times 1$ vector containing the receive path gain for each tile, $\sigma_{\rm cal} = \mathcal{E}\left\{s(t)s^H(t)\right\}$ is the power of the calibration source and $\sigma_{\rm n}$ is the noise power in an individual antenna, which is assumed equal for all antennas in the station.

As can be seen in (3), the measured correlations are directly proportional to the gains that we need to calibrate if the SNR is sufficiently high. The proportionality constant is related to the signal from the reference beam. The output power of the reference beam can be obtained by its autocorrelation $\widehat{r}_{yy}$, which has expected value

$$\begin{aligned} r_{yy} &= \mathcal{E}\left\{y(t) y^H(t)\right\} \\ &= \left|\mathbf{w}_{\rm ref}^H \mathbf{g}\right|^2 M^2 \sigma_{\rm cal} + \left(\mathbf{w}_{\rm ref}^H \mathbf{w}_{\rm ref}\right) M\sigma_{\rm n}. \end{aligned} \quad (4)$$

Dividing $\mathbf{r}$ given in (3) by r_{yy} given in (4), we get

$$\frac{\mathbf{r}}{r_{yy}} = \mathbf{g}\frac{\mathbf{g}^H \mathbf{w}_{\rm ref} M^2 \sigma_{\rm cal} + M\sigma_{\rm n}\mathbf{w}_{\rm ref}}{\left|\mathbf{w}_{\rm ref}^H \mathbf{g}\right|^2 M^2 \sigma_{\rm cal} + \left(\mathbf{w}_{\rm ref}^H \mathbf{w}_{\rm ref}\right) M\sigma_{\rm n}}. \quad (5)$$

If the weights of the reference beam are chosen such that $\mathbf{w}_{\rm ref} = \mathbf{1}/P$ and the gains can be modeled as $\mathbf{g} = \mathbf{1} + \boldsymbol{\epsilon}$, where $\boldsymbol{\epsilon}$ is a $P \times 1$ vector describing the deviation of the gains from their nominal value of unity, (5) can be written as

$$\frac{\mathbf{r}}{r_{yy}} = \mathbf{g}\frac{\left(1 + \boldsymbol{\epsilon}^H \mathbf{1}/P\right) M^2 \sigma_{\rm cal} + M\sigma_{\rm n}\mathbf{1}/P}{\left|1 + \boldsymbol{\epsilon}^H \mathbf{1}/P\right|^2 M^2 \sigma_{\rm cal} + M\sigma_n/P}. \quad (6)$$

The factor $\boldsymbol{\epsilon}^H \mathbf{1}/P$ represents the average deviation of the gains from their nominal value. If those errors are randomly distributed, which is a reasonable assumption given the fact that a common gain factor can be absorbed in $\sigma_{\rm cal}$, and these errors are small or the number of tiles is large, this factor will tend towards zero. This will then result in

$$\frac{\mathbf{r}}{r_{yy}} \approx \mathbf{g}. \quad (7)$$

If the condition $\epsilon^H \mathbf{1}/P << 1$ is not met, the gain estimate obtained from $\mathbf{g} = \mathbf{r}/r_{yy}$ will hopefully be more accurate than the assumption that all gains are identical, i.e., that $\mathbf{g} = \mathbf{1}$. We can then follow an iterative approach using $\mathbf{w}_{\rm ref} = \mathbf{1} \oslash \overline{\mathbf{g}_0}/P$, where $\oslash$ denotes element-wise division and $\mathbf{g}_0$ denotes the current best gain estimate. Our new gain estimate will then become

$$\frac{\mathbf{r}}{r_{yy}} = \mathbf{g}\frac{\frac{M^2\sigma_{\rm cal}}{P}\sum_{p=1}^{P}\frac{\overline{g_p}}{\overline{g_{0,p}}} + \frac{M\sigma_{\rm n}}{P}\mathbf{1} \oslash \overline{\mathbf{g}_0}}{\frac{M^2\sigma_{\rm cal}}{P^2}\left|\sum_{p=1}^{P}\frac{g_p}{g_{0,p}}\right|^2 + \frac{M\sigma_{\rm n}}{P^2}\sum_{p=1}^{P}\frac{1}{|g_{0,p}|^2}}. \quad (8)$$

Note that all summations provide a measure of the average gain variation or average gain difference. If, after a number of iterations, the initial estimate used to form the reference beam $\mathbf{g}_0$ converges to the true gain value $\mathbf{g}$, $\sum_{p=1}^{P} g_p/g_{0,p}$ converges to P. This will make the first term in both the numerator and the denominator converge to $M^2\sigma_{\rm cal}$. If this term is dominating the noise-related term, which is true if the SNR is high enough, $\mathbf{r}/r_{yy}$ will converge towards the true value of the gain vector $\mathbf{g}$. If the noise-related terms are not negligible, this will cause a bias in the estimated gain vectors. The impact of this bias will be assessed in more detail in the simulations in the next section.

2.3 Computational complexity

Standard calibration schemes require the array covariance matrix to be computed, which requires $4P^2\Delta\nu$ operations, where $\Delta\nu$ is the correlated bandwidth [5]. Calibration using an Alternating Direction Implicit (ADI) method usually requires significantly fewer operations [6]. The proposed method requires a beamformer to form the reference beam, which requires $8P\Delta\nu$ operations [5], followed by correlation of all tile signals with the reference beam signal and correlation of the reference beam signal with itself, which requires $4(P+1)\Delta\nu$ operations. If $N_{\rm iter}$ iterations are needed, the total number of operations grows to $N_{\rm iter}\Delta\nu\,(12P+4)$. As the gains usually vary smoothly and can be tracked during an observation, $N_{\rm iter}$ will usually be quite small, making the proposed method computationally attractive when P is large.

3 SIMULATION RESULTS

As the MFAA system is still in its design phase, different array designs are currently being evaluated

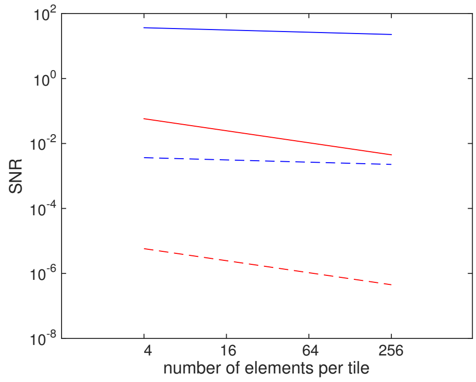

Figure 1: SNR with which $\mathbf{r}/r_{yy}$ can typically be measured before (dashed blue line) and after (solid blue line) integration over 10 MHz and 10 s. The red lines show the corresponding SNR values for a single antenna element in the array.

[3]. For the simulations in this paper, I will assume a dense configuration with antennas placed on a regular grid with a pitch of 0.125 m. As the number of tiles, P, in a station consisting of a fixed number of antennas, N, has a significant impact on the gain estimation bias described in (6) and (8), I will use $M \in \{4, 16, 64, 256\}$ to assess the impact of tile size. Note that $M = 256$ implies a 16×16-element tile, which already is 2 m on a side when the pitch is 0.125 m. This already violates the field-of-view requirement of 200 sq. deg. [3] for the highest frequencies, so there is no need to explore even larger values for M. To ensure an integer number of tiles, I choose $N = 100,096$, which results in a station diameter of about 44.6 m. I assume the same system temperature $T_{\mathrm{sys}} = 35$ K as in [3].

If the station needs to be calibrated during normal operation, calibration should be done using one of the sources inside the FoV of the tile as calibration source. A larger tile has a smaller beam and, therefore, the typical flux of the brightest source inside the tile beam will be lower. However, a larger tile also has a larger collecting area and, hence, a higher sensitivity. Figure 1 shows the SNR with which $\mathbf{r}/r_{yy}$ can be measured as function of tile size before and after integration over 10 MHz and 10 s based on the source statistics collected in [7]. As $\sigma_{\mathrm{n}} = \sigma_{\mathrm{cal}}/\mathrm{SNR}_{\mathrm{elem}}$, where $\mathrm{SNR}_{\mathrm{elem}}$ is the SNR for a single element in the array before integration, the SNR for the individual antenna elements is also plotted. This SNR determines the ratio of the signal and noise term in the numerator and denominator of (6) and (8). While the slope for the SNR per element is solely determined by the effect of the growing FoV as the sensitivity of an individual element does not depend on tile size, the SNR of the measurement does depend on both factors. Interestingly, this results in a very weak dependence on tile size, i.e, the accuracy with which we can determine $\mathbf{r}/r_{yy}$ mainly depends on the sensitivity of the station and the amount of integration over bandwidth and time that we can afford.

As the SNR per element before integration is very low, the noise term in the numerator (and denominator) in (6) and (8) is not negligible compared to the signal term. As this term also depends on the gain deviations, the simulations were set up as a Monte Carlo simulation in which the true gains were modeled as $g_p = 1 + \mathcal{CN}(0, 0.1)$, i.e., as zero mean Gaussian noise on the real and imaginary part with a standard deviation of 0.1 added to a nominal value of unity. For each choice of M, 100 realizations of the true gains were calibrated by applying (5) up to 20 times updating $\mathbf{w}_{\mathrm{ref}}$ after every iteration. This simulation was done using expected values for the correlations instead of emulating an actual (noisy) measurement as this isolates the effect of the bias described by (6) and (8) from the effect of the SNR of the measurement, which will likely be very good as indicated by Figure 1.

Figure 2 shows the convergence of the gain amplitudes and phases to their true values. These plots show that the average absolute difference between the estimated gain amplitudes and the true ones converges to a fixed value indicating a bias. For the phase solutions, the mean absolute difference between true and measured values converges steadily to zero. In both cases, the speed of convergence increases if the amplitude of the noise term in the numerator (and denominator) in (6) and (8) decreases relative to the amplitude of the signal term. The gain amplitude solutions appear to oscillate while converging to their final value. This behaviour has also been observed in gain calibration based on the ADI method [6], where it was demonstrated that the speed of convergence can be significantly improved by averaging the last two solutions every second iteration.

Figure 3 shows the gain amplitude and phase solutions obtained after 20 iterations for a representative run for $M = 4$. This plot explains the bias suggested by Fig. 2 for the gain amplitudes: the deviations of the gain amplitude solutions from the average gain amplitude value appear to be damped versions of the true deviations. A close inspection for all values of M indicates that the degree of damping is related to the ratio of the noise term and the signal term in the numerator (and denominator) in (6) and (8). This suggests that the estimates may be further improved by determining the SNR

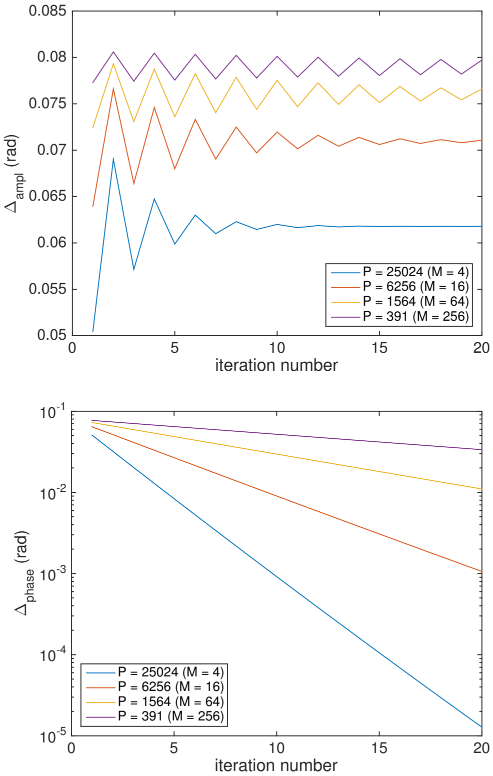

Figure 2: Mean absolute difference of the estimated gain values and the true gain values in terms of amplitude (top) and phase (bottom) after the indicated number of iterations.

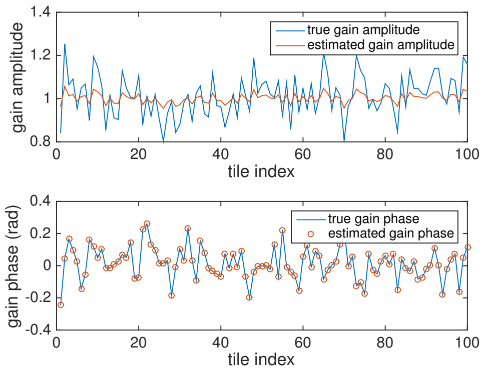

Figure 3: Comparison of the estimated gain amplitudes (top) and phases (bottom) with their true values for the first 100 tiles after the last (20th) iteration in a representative run.

of the calibration observation by additional measurements. The gain phase solutions have nicely converged to the true values. This implies that, without further improvements as indicated above, the proposed calibration method may cause a noisy aperture amplitude weighting but will produce a perfectly pointed beam.

4 CONCLUSIONS

In this paper, a self-holography method was proposed to calibrate arrays whose large number of receive paths make conventional calibration schemes based on the array covariance matrix computationally expensive or even infeasible. It was shown that the convergence rate increases with increasing SNR. The gain phases converge to the true values while the gain amplitude solutions exhibit a bias that increases with decreasing SNR. The results suggest an avenue to reduce this bias, which will be explored in a future study.

Acknowledgments

This work is supported by the Netherlands Organisation for Scientific Research.

References

[1] P. E. Dewdney *et al.*, "The Square Kilometre Array," *Proceedings of the IEEE*, vol. 97, no. 8, pp. 1482–1496, Aug. 2009.

[2] W. A. van Cappellen *et al.*, "MANTIS: The Mid-Frequency Aperture Array Transient and Intensity-Mapping System," https://arxiv.org/abs/1612.07917, Dec. 2016, MANTIS white paper.

[3] A. Faulkner, "Mid-Frequency AA Technology," in *3rd MIDprep / AA-mid workshop*, Cape Town, South Africa, 7-9Mar. 2016.

[4] A. R. Thompson, J. M. Moran, and G. W. Swenson Jr., *Interferometry and Synthesis in Radio Astronomy*, 3rd ed. Springer Open, 2017.

[5] R. Jongerius *et al.*, "An End-to-End Computing Model for the Square Kilometre Array," *IEEE Computer*, vol. 47, no. 9, pp. 48–54, Sep. 2014.

[6] S. Salvini and S. J. Wijnholds, "Fast gain calibration in radio astronomy using alternating direction implicit methods: Analysis and applications," *Astronomy & Astrophysics*, vol. 571, no. A97, pp. 1–14, Nov. 2014.

[7] J. D. Bregman, "System Design and Wide-field Imaging Aspects of Synthesis Arrays with Phased Array Stations," Ph.D. dissertation, University of Groningen, Groningen, The Netherlands, Dec. 2012.